A Platoon Regulation Algorithm to Improve the Traffic Performance of Highway Work Zones

(article starts on next page)

COMPUTER-AIDED CIVIL AND INFRASTRUCTURE ENGINEERING   WILEY

A platoon regulation algorithm to improve the traffic performance of highway work zones

Danni Cao[1] | **Jiaming Wu**[2,3] | **Jianjun Wu**[1] | **Balázs Kulcsár**[2] | **Xiaobo Qu**[3]

[1] State Key Laboratory of Rail Traffic Control and Safety, Beijing Jiaotong University, Beijing, China

[2] Department of Electrical Engineering, Chalmers University of Technology, Gothenburg, Sweden

[3] Department of Architecture and Civil Engineering, Chalmers University of Technology, Gothenburg, Sweden

Correspondence
Jiaming Wu, Chalmers University of Technology, Department of Electrical Engineering, Department of Architecture and Civil Engineering, SE-41296, Gothenburg, Sweden.
Email: jiaming.wu@chalmers.se

Jianjun Wu, State Key Laboratory of Rail Traffic Control and Safety, Beijing Jiaotong University, 100044, Beijing, China.
Email: jjwu1@bjtu.edu.cn

Funding information
Swedish Innovation Agency - Vinnova; HIEM; National Key R&D Program of China, Grant/Award Number: 2019YFB1600200; National Natural Science Foundation of China, Grant/Award Numbers: 71890972/71890970, 71621001, 71525002

Abstract
This paper presents a cooperative traffic control strategy to increase the capacity of nonrecurrent bottlenecks such as work zones by making full use of the spatial resources upstream of work zones. The upstream area is divided into two zones: the regulation and the merging areas. The basic logic is that a large gap is more efficient in accommodating merging vehicles than several small and scattered gaps with the same total length. In the regulation area, a nonlinear programming model is developed to balance both traffic capacity improvements and safety risks. A two-step solving algorithm is proposed for finding optimal solutions. In the merging area, the sorting algorithm is used to design lane-changing trajectories based on the regulated platoons. A case study is conducted, and the results indicate that the proposed model is able to significantly improve work zone capacity with minor disturbances to the traffic.

1 | INTRODUCTION

On highways, a work zone usually refers to a temporarily closed area where road construction or maintenance is underway. Existing studies show that work zones account for a large proportion of congestions on highways due to a reduced number of operational lanes (Chin et al., 2002; Chung & Recker, 2012). The capacity drop near work zones not only results in reduced traffic efficiency but also induces more traffic crashes (Han et al., 2020; Memarian et al., 2019; Z. Zheng et al., 2010; Z. Zheng, 2014; Zhou & Ahn, 2019; Z. Zheng & Sarvi, 2016). To address this problem, numerous studies have been conducted to improve the performance of work zones through various approaches, such as capacity drop and traffic delay prediction (H. Zheng et al., 2014; Jiang & Adeli, 2003, 2004a, 2004b), traffic flow prediction (Adeli & Ghosh-Dastidar, 2004; Hou et al., 2015), variable message sign techniques (Hooshdar & Adeli, 2004), merging strategy developments (Karim & Adeli, 2003), and feedback control (Papageorgiou et al., 2008).

In the 1990s, the automated highway system was widely studied to improve highway performance. Most of the related studies focused on capacity evaluation (Hall, 1995; Tsao et al., 1997) and control rules for platoon formation or split (Chien et al., 1995; Godbole & Lygeros, 1994;

Hall & Lotspeich, 1996) on normal lanes. With the development of connected vehicles (CVs), new treatments are now possible since vehicles can communicate in real-time through vehicle-to-vehicle or vehicle-to-infrastructure networks and thus drive more cooperatively than ever before (Xu et al., 2020; Z. Wang et al., 2020). One notable approach is to design cooperative lane-changing trajectories so that merging maneuvers can be performed more effectively.

A mandatory lane changing (MLC) is usually defined as a required task that must be performed to follow a specific route (Z. Zheng, 2014). With the assistance of the emerging cooperative vehicles, major MLC decision modeling approaches can be roughly classified into rule-based and optimization-based methods.

In rule-based methods, the basic idea is to coordinate mainline and ramp vehicles by certain rules so that they could drive through bottleneck areas smoothly. For instance, Ntousakis et al. (2016) proposed an automated procedure for cooperative vehicle merging considering the passenger comfort and engine effort in the on-ramp with one mainstream lane. Model inputs include the time to the merging point and the final speed for facilitating the merging procedure. Moreover, the methodology can also be applied through a model predictive control (MPC) scheme in case of a system error. Scarinci et al. (2017) used macroscopic and microscopic traffic flow theory to define a cooperative merging strategy, which describes the gap size for merging space and the time needed for creating the merging gap. The research inspires us to coordinate on-ramp vehicles with mainline gaps with the purpose of facilitating merging in a connected environment. Liu et al. (2018) extended a cooperative adaptive cruise control (CACC) modeling framework for car-following and lane-changing rules with both CACC-equipped and human-driven vehicles (HVs). The method includes various vehicle dispatching and human driver models, making it possible to reproduce the traffic dynamics in multilane highways.

Optimization-based approaches seek to optimize merging trajectories for various vehicles subject to certain constraints. Letter and Elefteriadou (2017) designed a merging algorithm to maximize average travel speed (ATS) for connected and automated vehicle platoons on the mainline and one-ramp lane. It revealed that in uncongested conditions the algorithm was able to reduce travel time, increase ATS, and improve throughput. Zhou et al. (2019) transformed the merging maneuvers task into two related optimal control problems, which are mainline facilitating and merging vehicle optimal control. The motivation of the proposed strategy was to restrain a facilitating maneuver's impact on the following traffic. Hu and Sun (2019) developed an online system control algorithm by optimizing vehicles' lane-changing and car-following trajectories.

The algorithm divided the ramp area into cooperative lane-changing and merging regions to deal with multilane merging problems. Jing et al. (2019) considered the global optimal merging problem as a cooperative game to achieve minimum values for the global pay-off conditions. The optimization problem was then decomposed into multiple two-player games. Fuel consumption, passenger comfort, and travel time within the merging control zone were used as the pay-off conditions. Ali et al. (2019) also applied the game theory for modeling the comprehensive MLC models in both the traditional environment and the CV environment. The model showed high accuracy in replicating observed MLC behavior and achieved minimum values for the global pay-off conditions. Wu et al. (2020) proposed a pre-clearing strategy to prioritize emergency vehicles by developing an optimal trajectory for surrounding CVs. Chen et al. (2020) proposed a hierarchical control approach to facilitate the merging of CVs on ramps. A tactical layer controller applying a second-order car-following model and an operation layer based on MPC are combined to minimize an objective function for different time horizons. The limitation is that their method can only be applied to a merging area with one main lane. Duret et al. (2020) also applied the two-layer controllers in splitting a platoon of vehicles approaching an on-ramp. The results showed the method guaranteed the possibility of forming the platoon under safe conditions. Instead of setting control areas upstream of the merging area, this study combined the car-following model with the predictive control to find the optimal trajectory for each vehicle.

In addition, many studies have attempted to improve the traffic performance upstream of the work zone by adjusting the location of traffic signs, which can be generally classified into early merge (EM) and late merge (LM) strategies. The overarching idea of EM is to encourage vehicles to execute merging before approaching the work zone, thus reducing forced merges to improve efficiency (Tarko et al., 1998; Yang et al., 2009). For LM, vehicles are encouraged to use both the blocked and normal lanes until they reach the merging point (Beacher et al., 2004; Kang & Chang, 2009; McCoy & Pesti, 2001). However, EM may increase the travel time and delay as the vehicles are forced to merge into one lane far away from the work zone. Moreover, LM may have safety issues for all the vehicles on the blocked lane to change their lane near the work zone.

In summary, there are three notable limitations in most existing studies. First, most MLC studies adopted the passive control approach to moderate merge demand, especially under overloaded demand. Proactive approaches to avoid a system failure in advance are rare in the literature. Second, most studies such as EM or LM only focus on either efficiency or safety. A more integrated study is necessary considering both efficiency and safety issues. Third,
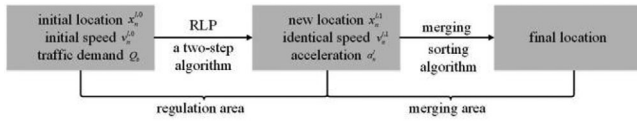
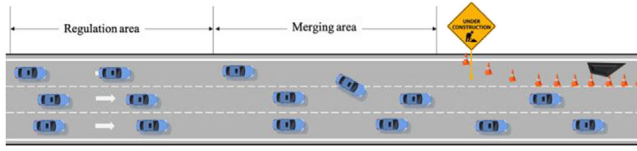**FIGURE 1** The technical scheme of the present paper

FIGURE 2 Schematic layout of the emergency area

most studies in the connected traffic environment address recurrent bottlenecks at fixed locations such as highway ramps or weaving sections, where pre-solutions are determined. At nonrecurrent bottlenecks such as work zones or crash sites, such treatments are not practical, where there is a need for flexible strategies that could adapt to sporadic emergency scenarios.

To this end, in this paper, we propose a cooperative control strategy for work zones, aiming to improve the traffic performance in such areas through proactive regulations and cooperative driving in a connected environment. Figure 1 illustrates the technical scheme of the present paper, which can be applied to typical work zones as illustrated in Figure 2. For convenience, the blocked lane in work zones or crash sites will be referred to as the blocked lane and other lanes as the normal lanes. The gaps mentioned in this research indicate distance headway. The proposed control strategy includes two stages, that is, the regulation stage and the merging stage. In the regulation stage, a nonlinear programming model is developed to adjust longitudinal positions of vehicles on the normal lanes with the purpose of accommodating more merging vehicles. Specially, we notice the fact that vehicles driving in platoons usually result in a smaller average gap, indicating that a large vehicle gap on normal lanes is more efficient in accommodating merging vehicles than several small and scattered gaps with the same total length. In other words, we seek to moderately reform several small gaps into large gaps so that vehicles could naturally drive with smaller gaps due to platooning, instead of directly controlling headways. We propose a regulation longitudinal position (RLP) model to adjust vehicular positions on normal lanes to create larger gaps for merging as well as minimizing the introduced disturbance on those vehicles. Subsequently, with the regulated gaps, we develop an optimal control strategy in the merging stage to design optimal merging trajectories for all vehicles.

In the merging stage, we apply the sorting algorithm to design optimal trajectories for vehicles in both the blocked and normal lanes to complete the merging process with minimum costs. The two-stage model is mainly developed to relieve congestions at nonrecurrent bottlenecks and certainly also be applied to promote operational performance in recurrent bottlenecks.

The remainder of the paper is arranged as follows: Section 2 will introduce the assumptions and the nonlinear model for the proposed control method; Section 3 illustrates a new gradient descent algorithm to solve our nonlinear programming model; Section 4 presents a case study to demonstrate the proposed control method; and Section 5 concludes the paper with discussions.

2 | METHODOLOGY

This section elaborates on the proposed models including the RLP model applied in the regulation area and the merging control model used in the merging area. For the simplicity of tracking notation, we summarize all of the notations in Table 1 for convenience.

2.1 | RLP model

The work zone area features a reduced capacity due to lane closure. When traffic volume exceeds capacity near the work zone, it will contribute to flow breakdown and lead to congestion that causes capacity drop. To avoid breakdown and facilitate the merging before lane reduction point and maintain capacity, we here propose the RLP model to moderately make the vehicles more compact on normal lanes so that larger lane-changing gaps could be created to accommodate more merging vehicles. Details of the RLP model will be elaborated later in this section.

2.1.1 | Objective function

In this study, the following assumptions are made: (1) the initial position and speed of each vehicle are known; (2) before all vehicles in the normal lanes reach an identical speed, they adjust longitudinal positions with the constant acceleration/deceleration; (3) the length of the regulation area and merging area are fixed; (4) all vehicles will comply with the designed trajectories. In our research, the regulation area length is crucial but depends on various factors such as the optimal time, the traffic demand, and the lane width. To focus on the key problem of vehicle cooperation, we here assume a fixed length of the regulation area.

In the RLP model, we mainly consider two objectives: (1) minimizing safety risks; (2) maximizing capacity

TABLE 1 Notation list

n	Index of the vehicles on any lane
l	Index of the lanes
c_n^l	The index of vehicle n on lane l
r_n^l	The change of the relative distance between vehicle n and its upstream neighboring $n + 1$ on lane l after the regulation longitudinal position (RLP)
$s_n^{l,0}$	Number of vehicles that can merge into the gap between vehicle n and its upstream neighboring $n + 1$ on lane l before the RLP
$s_n^{l,1}$	Number of vehicles that can merge into the gap between vehicle n and its upstream neighboring $n + 1$ on lane l after the RLP
$v_n^{l,0}$	Speed of the vehicle n on lane l before the RLP
$v_n^{l,1}$	Speed of the vehicle n on lane l after the RLP
a_n^l	The acceleration rate of vehicle n on lane l during the RLP
t_n^l	Time for acceleration/deceleration during the RLP of vehicle n on lane l
Δt_n^l	The time difference to complete the acceleration or deceleration between vehicle n and its upstream neighboring $n + 1$ on lane l
y_n^l	The travel distance of the vehicle n on lane l during the RLP
$x_n^{l,0}$	The location of vehicle n on lane l before the RLP
$x_n^{l,1}$	The location of vehicle n on lane l after the RLP
$d_n^{l,0}$	The available distance gap between vehicle n and its upstream neighboring $n + 1$ on lane l before the RLP
$d_n^{l,1}$	The available distance gap between vehicle n and its upstream neighboring $n + 1$ on lane l after the RLP
d_{min}	The security longitudinal distance between a vehicle and its upstream neighboring on the same lane
T_{max}	The total travel time used in the RLP
Q_b	The total number of vehicles on the blocked lane
R_n^l	The absolute value of the relative moving distance between vehicle n and its upstream neighboring $n + 1$ on lane l after the RLP
$B_n^{l,j}$	Binary variable to determine the value of the piecewise constant nondecreasing function
ω	The weighting factor of the capacity term for different priority needs in optimization
v_{max}	The maximum vehicle speed
v_{min}	The minimum vehicle speed

improvement. Decision variables in the optimization problem include the speed $v_n^{l,1}$ of vehicle n on lane l after the regulation stage and the acceleration rate a_n^l of vehicle n on lane l during the regulation stage. Safety and capacity are two crucial objectives when vehicles are driving near the emergency area. In our research, the regulation of gaps can be seen as a disturbance to normal traffic, which may induce conflicts and increase crash risk. The disturbance

is measured by the change of distance r_n^l between a vehicle pair (here, we use vehicle pair to indicate a vehicle n and its upstream neighboring vehicle $n + 1$ on the same lane) due to the regulation as shown in Equation (1) in which the sum of $|r_n^l|$ represents disturbances to the normal traffic:

$$F_1 = \min \left(\sum_{l=1}^{L} \sum_{n=1}^{N_l} |r_n^l| \right) \quad (1)$$

Since a large gap on normal lanes is more efficient in accommodating merging vehicles than several small and scattered gaps with the same total length, we measure the increased capacity by counting the increased number of vehicles on the blocked lane that can merge into the normal lane. After rearranging vehicles on the same lane, some small gaps are combined into big ones between vehicle pairs, which provide enough space for vehicles to merge. Therefore, we optimize the capacity improvement by maximizing the sum of increased gaps between any vehicle pair:

$$F_2 = \max \left(\sum_{l=1}^{L} \sum_{n=1}^{N_l} s_n^{l,1} - \sum_{l=1}^{L} \sum_{n=1}^{N_l} s_n^{l,0} \right)$$

$$= \min \left(\sum_{l=1}^{L} \sum_{n=1}^{N_l} s_n^{l,0} - \sum_{l=1}^{L} \sum_{n=1}^{N_l} s_n^{l,1} \right) \quad (2)$$

With both safety and capacity taken into consideration, an objective function is defined with Equation (3) in which ω is the weighting factor of the capacity term for different priority needs in optimization. Detailed explanations of ω will be introduced in Section 4:

$$F = F_1 - \omega F_2$$

$$= \min \left(\sum_{l=1}^{L} \sum_{n=1}^{N_l} |r_n^l| - \omega * \left(\sum_{l=1}^{L} \sum_{n=1}^{N_l} s_n^{l,1} - \sum_{l=1}^{L} \sum_{n=1}^{N_l} s_n^{l,0} \right) \right) (3)$$

2.1.2 | Constraints

As illustrated in former studies (Castillo-Manzano et al., 2019; Choudhary et al., 2018; Matírnez et al., 2013; Sun et al., 2018; X. Wang et al., 2016; X. Wang et al., 2018), the speed variation of vehicle pairs will increase the crash risk. In addition, to keep the relative distance $d_n^{l,1}$ stable after the regulation stage, one constraint in our research is that all vehicles on the normal lanes have the identical speed $v_n^{l,1}$ to enter into the merging area. Other constraints are developed mainly considering three aspects, including: (1) vehicle dynamic, which describes the longitudinal behavior of each vehicle; (2) safety constraints,

which guarantees the minimum distance between a vehicle pair; (3) capacity improvements, which guarantees that the merging demand due to work zones can be accommodated after regulation.

(1) Vehicle dynamic

In this paper, we assume that each vehicle in the regulation area executes either uniform acceleration or deceleration motion to reach the identical speed $v_n^{l,1}$, respectively. For a single vehicle, the speed before and after the RLP is $v_n^{l,0}$ and $v_n^{l,1}$, respectively. As a result, each vehicle on the normal lane needs t_n^l to achieve the desired identical speed as follows:

$$t_n^l = \frac{v_n^{l,1} - v_n^{l,0}}{a_n^l} \tag{4}$$

$$v_{\max} \leq v_n^{l,1} \leq v_{\min} \tag{5}$$

If the vehicle does not need to execute acceleration or deceleration, it will cruise at a constant speed $v_n^{l,1}$ during the whole RLP.

The variety of a_n^l and $v_n^{l,0}$ contributes to different t_n^l for acceleration or deceleration. As a result, the time difference Δt_n^l between a vehicle pair during the regulation stage can be obtained:

$$\Delta t_n^l = t_n^l - t_{n+1}^l \tag{6}$$

To ensure that the regulation can be completed in time before the lane reduction point, we set up a time threshold $T_{\max}$, which is the maximal regulation time:

$$t_n^l \leq T_{\max} \tag{7}$$

After the regulation stage, all the vehicles on the normal lanes have the identical speed of $v_n^{l,1}$. However, since the acceleration (deceleration) time t_n^l for each vehicle is different, vehicles with longer regulation time may execute either uniform acceleration or deceleration motion first, and then travel at the constant speed $v_n^{l,1}$ until all the vehicles in the regulation area cruise with $v_n^{l,1}$. Therefore, the travel distance yy_n^l consists of two parts, that is, the uniform acceleration (deceleration) part and the constant speed part, which are modeled as follows:

$$v_n^{l,1} = v_{n+1}^{l,1} \tag{8}$$

$$y_n^l = \frac{\left(v_n^{l,1}\right)^2 - \left(v_n^{l,0}\right)^2}{2*a_n^l} + T_{\max} - t_n^l * v_n^{l,1} \tag{9}$$

$$y_{n+1}^l = \frac{\left(v_{n+1}^{l,1}\right)^2 - \left(v_{n+1}^{l,0}\right)^2}{2*a_{n+1}^l} + T_{\max} - t_{n+1}^l * v_{n+1}^{l,1} \tag{10}$$

(2) Safety constraints

To avoid traffic conflicts, a safety distance should always be maintained between a vehicle pair in the longitudinal direction during regulation as defined in Equations (11) and (12):

$$d_n^{l,0} \geq d_{\min} \tag{11}$$

$$d_n^{l,1} \geq d_{\min} \tag{12}$$

Although safety distance may depend on the speed of vehicles, we assume a constant length $d_{\min}$ as the safety distance to facilitate modeling and solution development. Since the cooperative driving concept is adopted in this study, we believe that a uniform safety distance can be a reasonable simplification because each vehicle is aware of other vehicles' movements, which could largely reduce the risk of conflicts.

(3) Capacity improvements

In our research, the merging capacity is increased by regulating the longitudinal distance between different vehicles. The relative moving distance between vehicle n and its upstream neighboring $n + 1$ on lane l after the regulation stage can be obtained by the travel distance of a vehicle pair:

$$r_n^l = y_n^l - y_{n+1}^l = \frac{\left(v_n^{l,1}\right)^2 - \left(v_n^{l,0}\right)^2}{2*a_n^l} - \frac{\left(v_{n+1}^{l,1}\right)^2 - \left(v_{n+1}^{l,0}\right)^2}{2*a_{n+1}^l}$$
$$- \Delta t_n^l * v_n^{l,1} \tag{13}$$

The available gap between a vehicle pair before and after the regulation stage is according to the initial location and the relative moving distance, respectively:

$$d_n^{l,0} = x_n^{l,0} - x_{n+1}^{l,0} \tag{14}$$

$$d_n^{l,1} = d_n^{l,0} + r_n^l \tag{15}$$

With a larger distance between a vehicle pair, the number of vehicles that can merge into the gap increases. The number of vehicles that can merge into a gap of length $d_n^{l,1}$ can be seen as a function of the gap length. In addition, a fact is that in the merging area, the average gap occupied
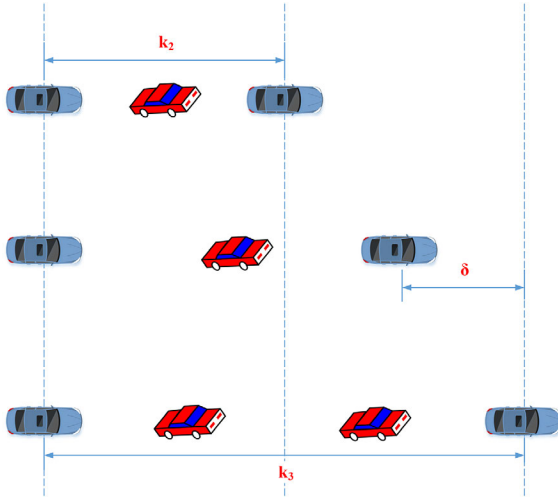
FIGURE 3 The illustration for accommodating vehicles

FIGURE 4 FThe sorting algorithm

by a vehicle is smaller in larger gaps than that in smaller gaps.

The mentioned phenomenon is illustrated in Figure 3. It is assumed that the minimum gap $d_n^{l,1}$ to accommodate one vehicle is k_2, while when the $d_n^{l,1}$ changes from k_2 to $k_3 - \sigma$ (where σ is infinitesimal to ensure the inter-vehicle space cannot accommodate two vehicles), the gap still can only accommodate one vehicle. When the former vehicle moves ahead σ meters longer than the later vehicle, the $d_n^{l,1}$ can then accommodate two vehicles. Therefore, the average gap occupied in larger gaps by a vehicle is smaller than that in smaller gaps.

To estimate the increased capacity during the RLP, we here design a piecewise constant nondecreasing function to map the gap length to merge capacities according to the average gap. Without loss of generality, we assume that the function is divided into $p + 1$ segments as Equation (16)

$$ s_n^{l,1} = \begin{cases} 0 & k_1 \le d_n^{l,1} < k_2 \\ 1 & k_2 \le d_n^{l,1} < k_3 \\ \vdots \\ p-1 & k_p \le d_n^{l,1} < k_{p+1} \\ p & k_{p+1} \le d_n^{l,1} \end{cases} \tag{16} $$

where $k_1, k_2, \dots k_p, k_{p+1}$ are threshold values of gaps.

To ensure that all of the vehicles on the blocked lane can merge into the normal lane, the sum of $s_n^{l,1}$ on the normal lanes must be larger than the traffic demand on the blocked lanes as defined in Equation (17):
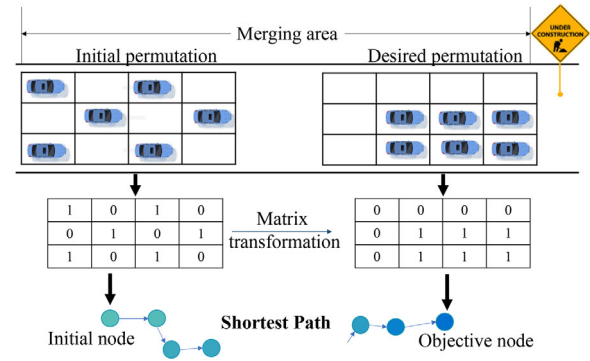
$$ \sum_{l=1}^{L} \sum_{n=1}^{N} s_n^{l,1} \ge Q_b \tag{17} $$

We would like to note that, in this step, the vehicles on the blocked lane are not directly assigned to the created gaps. The major reason is that such a mapping procedure indicates solving the regulation problem and the matching (vehicle-to-gap) problem simultaneously, which both are NP-hard problems. Solving several NP-hard problems simultaneously can be very challenging and even intractable in practice. Moreover, we believe that creating as many gaps as possible for merging vehicles is a more robust and possibly safer approach, compared with assigning each vehicle explicitly to a gap that needs to be created, especially in unexpected cases such as when there are more merging vehicles coming.

2.2 | Merging control model

After longitudinal regulations, the normal lanes are well prepared with larger feasible lane-changing gaps, and the subsequent issue is how and when vehicles on the work zone lane merge into normal lanes. Here, we applied the sorting algorithm (Wu et al., 2020), which could find optimal trajectories to transform a multi-lane vehicular platoon from any permutation to any desired permutation through cooperative driving.

A brief introduction of the sorting algorithm is presented as shown in Figure 4. In the sorting algorithm, we first discretize the vehicle platoon as a grid system, which is further modeled with a matrix presentation. The problem of cooperative merging is then converted to a problem of matrix transformation, following practical rules of vehicle movements. Subsequently, each matrix that denotes a permutation of the vehicle platoon is considered as a vertex in a graphic domain. Following this logic, finding the optimal trajectories to complete the merging is equivalent to finding the shortest path between the initial and objective nodes in the graphic domain, which can be easily solved by many existing path-finding algorithms. Note that in each movement step, a vehicle can only move to an adjacent

3 | SOLVING ALGORITHM

In this section, we develop a two-step algorithm to improve the operation in the regulation area and provide a brief introduction of the sorting algorithm applied in the merging area.

3.1 | A two-step solving algorithm for the regulation model

In the regulation stage, both $v_n^{l,1}$ and a_n^l are decision variables, and the problem has been formulated as a nonlinear programming problem with the objective function of Equation (3) and constraints from Equations (4) to (17). In the two-step solving algorithm, in order to simplify the model, we first perform the following transformation on the original model:

(1) Linearize the objective function.

The existence of absolute values in the objective function complicates the model, and we introduce a new variable R_n^l, which satisfies

$$R_n^l \geq r_n^l \tag{18}$$

$$R_n^l \geq -r_n^l \tag{19}$$

Then, the objective function can be derived as

$$F = \min\left(\sum_{l=1}^{L}\sum_{n=1}^{N_l} R_n^l - \omega*\left(\sum_{l=1}^{L}\sum_{n=1}^{N_l} s_n^{l,1} - \sum_{l=1}^{L}\sum_{n=1}^{N_l} s_n^{l,0}\right)\right) \tag{20}$$

(2) Linearize the piecewise constant nondecreasing function.

We introduce $p + 1$ binary variables $B_n^{l,j}$ $(j = 0, 1, 2, \ldots, p-1, p)$, and set the binary matrix B as

$$B = \left[B_n^{l,0}, B_n^{l,1}, B_n^{l,2}, \ldots, B_n^{l,P-1}, B_n^{l,P}\right] \tag{21}$$

The piecewise constant nondecreasing function can be explained in Equations (22) to (25):

$$\sum_{j=0}^{p} B_n^{l,j} = 1 \tag{22}$$

$$s_n^{l,1} = B*[0, 1, 2, \ldots, (p-1), p]^T \tag{23}$$

$$d_n^{l,1} > B*\left[k_1, k_2, k_3, \ldots, k_{p+1}\right]^T \tag{24}$$

$$d_n^{l,1} \leq B*\left[k_2, k_3, \ldots, k_{p+1}, M\right]^T \tag{25}$$

where M is a big value.

We apply a two-step algorithm to solve this optimization model. The basic idea is to convert this nonlinear program model into a linear program model. For the $v_n^{l,1}$ is limited to a certain range upstream the work zone, we first use the gradient descent method to determine the $v_n^{l,1}$, and then only the a_n^l is unknown. As a result, we can regard the model as the linear program model.

In the gradient descent method, we use the first-order difference to replace the derivative for determining the descent direction:

$$\nabla F(v) = \frac{F(v + \Delta v) - F(v)}{\Delta v} \tag{26}$$

Then, the initial speed of the next iteration v_2 is

$$v_2 = v_1 - \gamma*\nabla F(v) \tag{27}$$

where v_1 is the speed of the former iteration, and γ is the step size and $\gamma \in R_+$.

The complete two-step algorithm used in the RLP to solve the optimization model is illustrated as follows:

Algorithm I Calculation of function value of Equation (20)

Random generate $v_n^{l,1}$ recorded in A
For $v_n^{l,1}$ in A **do**
  Repeat
    Obtain F with $v_n^{l,1}$ using Gurobi (Gurobi Optimization, Inc. 2014)
    Calculate $v_n^{l,1'}$, $v_n^{l,1'} = v_n^{l,1} - \gamma * \nabla F(v_n^{l,1})$
    Obtain F′ with $v_n^{l,1'}$
    Calculate ε, $\varepsilon = |F' - F|$
    Update $v_n^{l,1}$, $v_n^{l,1} \leftarrow v_n^{l,1'}$
    Update F, $F \leftarrow F'$
    If $\varepsilon < 0.01$
      Record $v_n^{l,1}$, F in set O
    End
  End
$v_n^{l,1\tilde{}} = \min(F(v_n^{l,1}))$, $v_n^{l,1} \in O$

3.2 | Sorting algorithm for merging

As described in Section 2.2, the problem of cooperative merging is converted to a problem of matrix transfor-

cell. More details can be found in the previous work of the authors (Wu et al., 2020).

TABLE 2 Optimization model parameter values designation

Parameter	Value	Parameter	Value	Parameter	Value	Parameter	Value
ω	10 (m/veh)	$d_{\min}$	10 (m)	Q_b	12 (veh)	$T_{\max}$	20 (s)

TABLE 3 Initial values of the model

Vehicle name	c_1^1	c_2^1	c_3^1	c_4^1	c_5^1	c_6^1	c_1^2	c_2^2	c_3^2	c_4^2	c_5^2	c_6^2	c_7^2
$x_n^{l,0}$	103	84	66	51	26	0	120	109	90	78	53	18	0
$d_n^{l,0}$	19	18	15	25	26		11	19	12	25	35	18	
$s_n^{l,0}$	0	0	0	1	1		0	0	0	1	2	0	
$v_n^{l,0}$	20.1	20.5	20.1	20.8	20.2	19.1	20.9	20.8	21	19.7	20.3	21.1	21.3

mation, where each node represents a permutation and each edge represents the "cost" associated with all vehicle movements to reach the permutation. To complete the merging operation, the solving process can be seen as finding the optimal trajectories for each vehicle to merge into the normal lanes. The basic logic of the sorting algorithm is adopted here to solve the cooperative driving problem based on the results of the regulation model. Unlike our previous work in Wu et al. (2020), which mainly addresses the vehicle platooning problem at signalized intersections, the objective in this study is to achieve a vehicular permutation in which all vehicles drive on the normal lanes. The Manhattan distance is used as the heuristic function when finding the shortest path in the modeled graph as shown in Figure 4. More details can be found in the previous work of the authors (Wu et al., 2020).

4 | CASE STUDY

In this section, a case study is provided to illustrate the proposed method. First, the proposed two-step algorithm is demonstrated for the regulation stage. We then investigate the influence of ω and T_{max} on capacity improvements. At last, we further explore the possibility of applying our algorithm to a framework to traffic demand management problems. Without loss of generality, in the case study, we assume a typical three-lane highway with a closed work zone occupying one lane as illustrated in Figure 2.

4.1 | Experiment setup

Ghiasi et al. (2017) concluded the headway distribution in different types of traffic including the traditional pure HVs, mixed vehicles, and pure automated vehicles (CAVs). It is summarized that the headway values between two HVs range from 0.7 to 2.4 s, and those between two CAVs range from 0.3 to 2 s. In our research, all of the vehicles are con-

nected and will drive cooperatively. Therefore, we select 0.5 s as the minimum headway between a vehicle pair on the same lane.

In our research d_{min} is set up as 10 m, and the piecewise constant nondecreasing function Equation (16) for vehicles on the blocked lane to merge into the normal lane is assumed to be

$$
s_n^{l,1} = \begin{cases}
0 & 0 < d_n^{l,1} < 20 \\
1 & 20 \le d_n^{l,1} < 30 \\
2 & 30 \le d_n^{l,1} < 40 \\
3 & 40 \le d_n^{l,1} < 50 \\
4 & 50 \le d_n^{l,1} < 60 \\
5 & 60 \le d_n^{l,1} < 70 \\
6 & 70 \le d_n^{l,1} < 80 \\
7 & 80 \le d_n^{l,1}
\end{cases}
\tag{28}
$$

For simplification, we only set Equation (16) as an eight-segment piecewise constant nondecreasing function. The specific formulation of Equation (16) can be flexibly adjusted in different conditions. The parameter ω is to balance the weight between the first and second terms in the objective function. In our case study, we consider capacity improvement and safety of equal importance. Since the incremental gap for accommodating an additional merging vehicle equals 10 m, ω is assumed to be equal to 10 m/veh. A list of the regulation stage model parameter values and initial values is shown in Tables 2 and 3.

4.2 | Results

The regulation model is optimized by the two-step algorithm introduced in Section 3. The optimal speed $v_n^{l,1}$ for the case study is found to equal 17.289 m/s, and the corresponding objective value is −63 m. Note that the objective function defined in Equation (3) is a weighted function that seeks to balance safety risks and improvements on
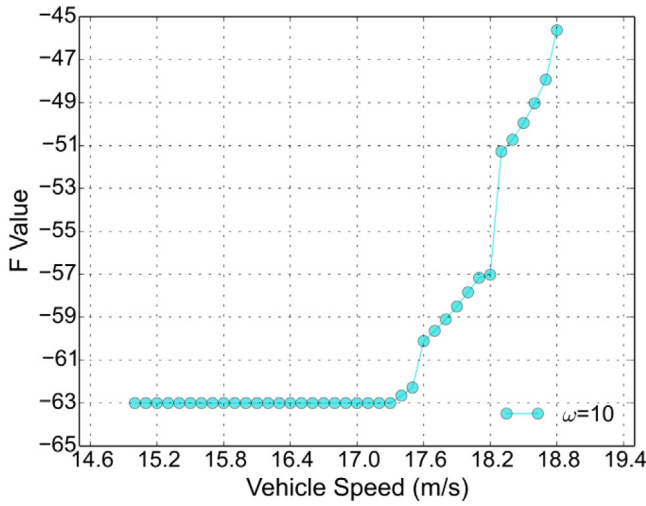
FIGURE 5 The objective function value of different $v_n^{l,1}$ with $\omega = 10$ m/veh

the storage capacity of gaps in normal lanes. A noteworthy problem is that with different initial values, the algorithm found the same optimal objective value with different optimal speed $v_n^{l,1}$. In such condition, we propose a method to determine the optimal speed $v_n^{l,1}$, with the objective to reduce the intensity of the disturbance by Equation (29), where v_{final}^i denotes the optimal speed in the ith iteration:

$$v_n^{l,1} = \arg\min_{v_{\text{final}}^i} \left(\sum_{l=1}^{2} \sum_{n=1}^{N_l} \left(v_{\text{final}}^i - v_n^{l,0} \right) \right) \quad i = 1, 2, 3 \dots I \tag{29}$$

It should be noted that the method of selecting the final speed could be adjusted according to the specific traffic scenario and other practical concerns, such as speed limit.

Table 4 shows the solution of the case study in the regulation stage. Before optimization, the vehicles on the normal lane only can accommodate five vehicles from the blocked lane to merge. After optimization, it can accommodate 17 vehicles within $T_{\max} = 20$ s. From Table 4, we can find that most vehicles first decelerate and then drive at a constant speed of $v_n^{l,1}$ to maintain the relative distance between a vehicle pair.

In order to verify the effectiveness of the two-step algorithm, we use the enumeration approach to find the globally optimal result. Since the model is nonlinear, we first enumerate the value of $v_n^{l,1}$, which ranges from 15 to 25 m/s with a step size of 0.1. Then the model is converted to a linear function with the decision variables a_n^l and can be solved by the Gurobi solver. After the enumeration, the relation between $v_n^{l,1}$ and the objective function value is presented in Figure 5. It shows that when the $v_n^{l,1}$ ranges from 14.8 to 17.3 m/s, the objective function achieves and maintains the minimum value of -63 m. When the iden-

TABLE 4 Solution for the case study

Vehicle name	c_1^1	c_2^1	c_3^1	c_4^1	c_5^1	c_6^1	c_1^2	c_2^2	c_3^2	c_4^2	c_5^2	c_6^2	c_7^2
$x_n^{l,1}$	469	449	419	399	369	339	491	471	451	431	401	361	341
$d_n^{l,1}$	20	30	20	30	30		20	20	20	30	40	20	
$s_n^{l,1}$	1	2	1	2	2	3	1	1	1	2	3	1	
a_n^l	0.14	0.19	0.27	0.65	0.93	3	0.2	0.26	0.3	0.2	0.46	1.5	2.83
t_n^l	19.6	16.5	10.3	5.4	3.1	0.6	18.2	13.6	12.3	12.3	6.5	2.5	1.4
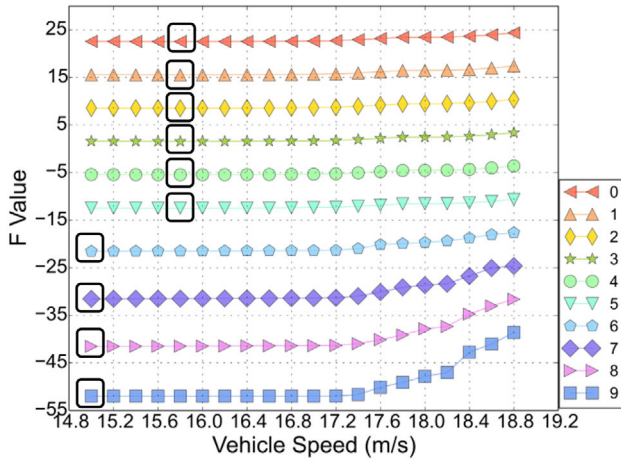
(a). ω various from 0 m/veh to 9 m/veh
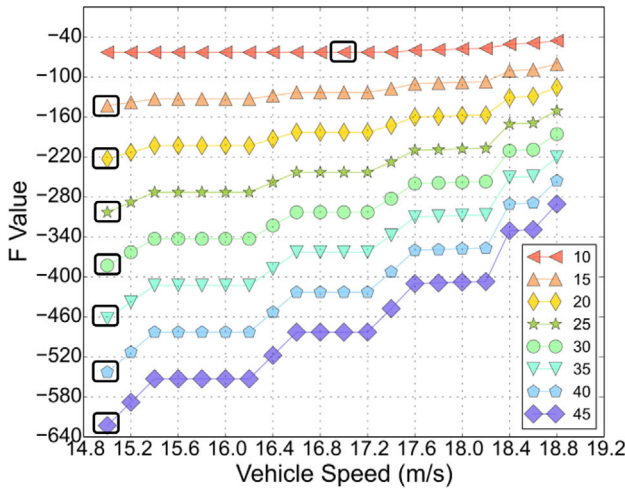
(b). ω various from 10 m/veh to 45 m/veh

FIGURE 6 The objective function value of different $v_n^{l,1}$ with various ω

FIGURE 7 The relation between the storage capacity of gaps and $T_{\max}$ with $v_n^{l,1} = 17.289$ m/s

tical speed is growing larger than 17.3 m/s, the value of the objective function increases significantly. Moreover, for the scenario with $\omega = 10$, the objective values are the same when the $v_n^{l,1}$ varies from 14.8 to 17.3 m/s. To reduce the intensity of the disturbance, $v_n^{l,1}$ is selected as 17.3 m/s, which is consistent with the results solved by the aforementioned two-step algorithm.

4.2.1 | Comparison against different weight coefficient

In this subsection, we explore how the weight factor ω affects optimal results. In Section 4.1, we grant equal priority to traffic safety and capacity for illustration. In practice, engineers and local authorities could use different ω for various traffic control objectives. Figure 6a shows how ω affects the optimal solution when ω ranges from 0 to
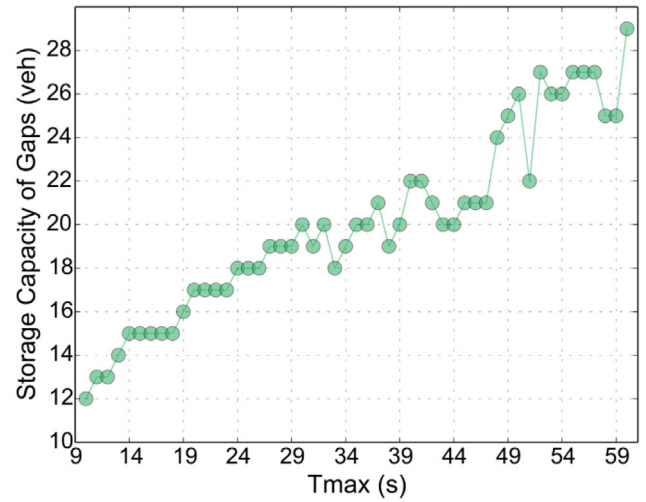
9 m/veh with 1 step size. The square marks the optimal $v_n^{l,1}$ for a specific value of ω. In certain orders of magnitude, with the decrease of ω, the optimal vehicle speed shows a piecewise increase. The results contribute to the decline of the relative speed variation before and after the RLP, which may reduce the intensity of the disturbance. It is also consistent with the realistic condition, as small ω means that the safety is more important, leading to smaller relative speed variation and thus less traffic risk. Figure 6b shows that the optimal vehicle speed is relatively stable when ω ranges from 10 to 45 m/veh. The reason is that the capacity term is dominating during optimization so that the optimal speed that mainly affects the safety term remains stable.

4.2.2 | Comparison against different total travel time

Now we explore when the optimal vehicle speed $v_n^{l,1}$ is 17.289 m/s, how different values of $T_{\max}$ affect the storage capacity of gaps measured by the number of vehicles that can fit in those gaps. Figure 7 indicates that with the increase of $T_{\max}$, the total storage capacity of gaps shows an upward trend. With longer regulation time, vehicles on the normal lanes have more time to adjust their longitudinal positions, and thus more storage capacity of gaps is produced. This finding could help the traffic management department to intuitively design a specific $T_{\max}$ or a certain length of regulation area for real-time traffic control based on the traffic demand.

While the $T_{\max}$ also affects the optimal speed result $v_n^{l,1}$, we set the $T_{\max}$ value of the RLP varying from 10 to 60 s with the step size 1 s. An interesting phenomenon is that as $T_{\max}$ increases, the storage capacity of gaps

TABLE 5   Simulation scenarios

Scenarios	Regulation	Available gaps	Num of vehicles	Num of samples
1	Before	5	5	30
2	After	17	5	30
3	After	17	6	30
4	After	17	7	30
5	After	17	8	30
6	After	17	9	30
7	After	17	10	30
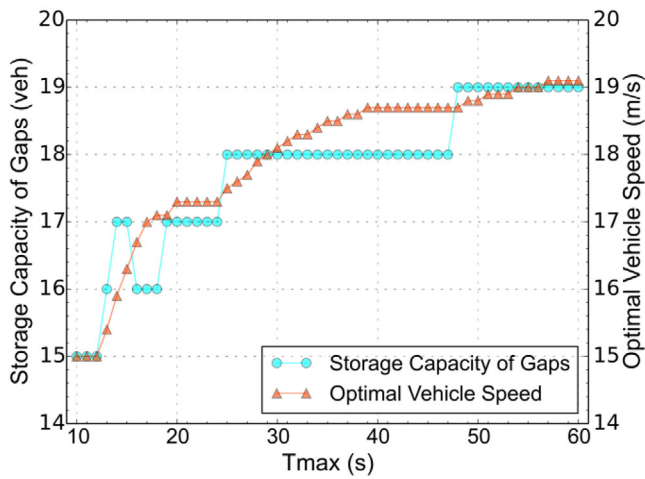
FIGURE 8   The relation between the storage capacity of gaps, $v_n^{l,1}$ and $T_{\max}$

FIGURE 9   The comparison of maneuver complexity between scenarios 1 and 2

does not increase infinitely but shows a modest growth as shown in Figure 8. With the increase of $T_{\max}$, the optimal $v_n^{l,1}$ becomes larger. The results also contribute to the decrease of the speed variation before and after the RLP, which reveals the improvement of the safety effect. The results reflect that our proposed RLP has the ability to adjust the relationship between the capacity and safety. With the larger $T_{\max}$, the storage capacity of gaps does not change a lot considering the mutually restrictive relation from the safety.

4.2.3 | The merging result

To investigate the benefits of the proposed method in facilitating merging maneuvers, we further examine the merging performance in various scenarios based on the initial setups in Table 3 and the regulation results in Table 4. Since the estimated merging demand is set up as 12 vehicles in this case study, theoretically, the regulated platoon could accommodate any merging demand with a platoon size smaller than 12. Therefore, seven scenarios are developed
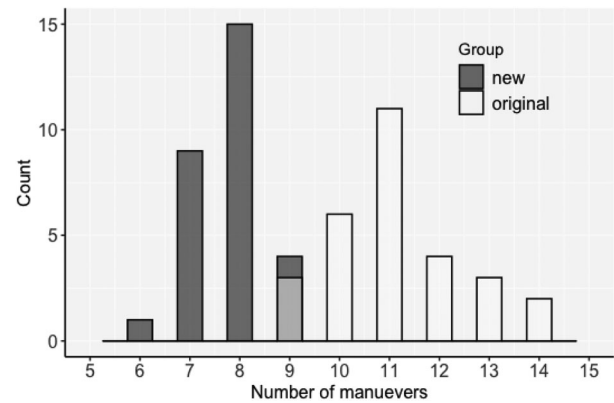
to compare the complexity of merging maneuvers under various merging demands as shown in Table 5.

Specifically, the minimal merging demand is set up as five vehicles, which can be just accommodated by the platoons on normal lanes before regulation. In addition, an increasing number of merging vehicles are examined where only the regulated platoon can serve the merging demand. For each scenario, we randomly generated 30 different initial permutations with a fixed number of merging vehicles, and for each permutation, the sorting algorithm is applied to find the optimal merging trajectories. In the present paper, we only focus on the complexity of merging behaviors, which is denoted by the total number of vehicle maneuvers, including accelerations/decelerations or lane-changing maneuvers.

Figure 9 presents the comparison of maneuver complexity between scenarios 1 and 2, entitled the original and new group, respectively. The figure implies that when serving the same number of merging vehicles, the regulated group clearly requires less vehicular maneuvers than the original group due to the increased number of usable gaps. This demonstrates that even when the original group could
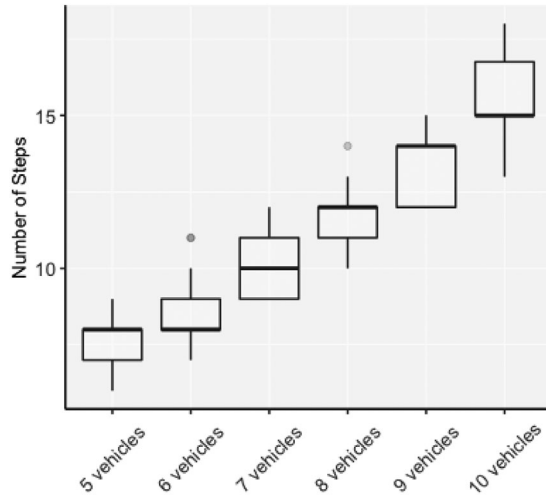
FIGURE 10 The comparison of maneuver complexity under various merging demand

accommodate all merging vehicles, the implementation of the regulation is still beneficial.

Figure 10 shows the number of vehicular maneuvers of the regulated platoon under various merging demands. It can be found that an increasing number of merging vehicles will also induce more merging maneuvers. Even though the result appears to be intuitive, this indicates a tradeoff between the storage capacity of gaps and maneuver complexity, which should not be ignored when making related decisions. However, this topic is beyond the scope of the present paper and needs more future work.

4.2.4 | Possible applications in traffic demand management

For traffic control, in reality, the application of different control models is still an important issue (Han et al., 2017). The proposed model here can be combined with the feedback control to coordinate the traffic condition upstream and downstream of the emergency area.

The feedback ramp metering algorithm ALINEA shown as Equation (30) can be applied in this research, which is based on the proportional-integral feedback control law (Papageorgiou et al., 1990).

$$q(k) = q(k-1) + k_R[\hat{o} - o(k-1)] \qquad (30)$$

where $k = 1, 2, \ldots$ is the time index; $q(k)$ is the entering flow during the new period k; $o(k-1)$ is the measured occupancy over the work zone area; $\hat{o}$ is the desired occupancy over the work zone area; and k_R is a regulator parameter.

In our research, the feedback control can be implemented according to Equations (31) and (32).

$$\sum_{l=1}^{L}\sum_{n=1}^{N} s_n^{l,1} = Q(k-1) + k_R[C - Q(k-1)] - Q_{non-o}(k) \qquad (31)$$

$$Q(k) = Q_o(k) + Q_{non-o}(k) \qquad (32)$$

where $Q(k)$ is the entering flow into the regulation area during the new period k; C is the desired traffic flow (capacity) of the lanes in the work zone area; $Q_{non-o}(k)$ is the entering flow of the normal lanes; and $Q_o(k)$ is the entering flow of the blocked lane.

When the emergency area is close to its capacity, the upstream of the regulation area should immediately improve the current control strategy to limit the traffic flow, such as the variable speed limit control. As a result, the established $s_n^{l,1}(k)$ in the RLP is adjusted according to the upstream and downstream traffic condition of the regulation area aiming at throughput maximization. It can facilitate the traffic management department to formulate reasonable traffic control measures in time when the emergency arrives.

4.3 | Comparison of different traffic volume

In order to further investigate the performance of the proposed control method, we here conducted comparative studies in different scenarios between the proposed methods and several existing strategies.

4.3.1 | Results evaluation with and without control measures

Here, we explore how the proposed method performs, compared with the traffic condition without control in different traffic volumes, which is completed by the state-of-the-art traffic simulation software Paramics. Fritzsche's model is applied in the car-following model in Paramics, which is based on a psychophysical model (Fritzsche, 1994). Specifically, it assumes that the driver can have one driving mode: Following I, following II, danger, closing in, and free driving (Brockfeld et al., 2003; Panwai & Dia, 2005). The input trajectory of our RLP is generated by the Paramics. We also compare our results with the basic scenario without control created in Paramics. In the experiments, the input volume varies from 1800 to 3000 vph with an increment of 600 vph on a three-lane highway with a closed work zone occupying the left, middle, and right

TABLE 6 Comparison of average travel speed (ATS) with and without control

Volume (vph)	Blocked lane	ATS (m/s)	
		Platoon	**Paramics**
1800	Left	23.07	25.60
2400	Left	21.02	19.84
3000	Left	18.29	6.67
1800	Middle	18.87	22.19
2400	Middle	16.38	7.65
3000	Middle	13.53	5.74
1800	Right	25.03	26.36
2400	Right	24.35	25.75
3000	Right	18.52	15.77

TABLE 7 Comparison of different control method

Volume (vph)	Mean travel time (s)				
	Platoon	**Paramics**	**Early merge**	**Late merge**	**New England Merge**
1200	100.4	101.2	115	112.1	114.2
1600	109.1	188.4	231.4	174.3	118.5
2000	112.7	252.7	484	482	189.8

lanes, respectively. To make the analysis realistic, 70% cars and 30% trucks are considered in the simulation. The speed is limited to 105 km/h. A notable thing is that in various traffic scenarios, the total length (TTL) of the regulation area and the sorting area is different. The ATS is selected as the measurement of performance, and the results are shown in Table 6. To avoid confusion, here the platoon regulation (denoted as "platoon" in Tables 6 and 7) indicates a control scenario with our proposed method, and the Paramics represents the scenario without control.

As shown in Table 6, in low traffic volume scenarios, the no-control group performs slightly better than the platoon regulation algorithm. A major reason is that, in the low traffic volume, vehicles are encouraged to accelerate to free flow speed in the simulation software and are able to smoothly perform lane changing in a natural way. While our method constrains that all vehicles need to follow the identical optimal speed. In the high traffic volume, the proposed algorithm presents improved efficiency, compared with the no-control group due to cooperative driving. When the high traffic density exceeds the one that achieves capacity, traffic flows become unstable and congested, leading to queueing upstream without control (Gartner et al., 2001). With different initial traffic condition, T_{max} may vary from nearly 10 to 50 s. In order to meet all merging demands, in each scenario, we choose the maximum T_{max} to facilitate the regulation. In the table, it can be found that the ATS in the control group does not change as dramatically as those in the no-control group. The reason is that vehicles are driving cooperatively and

are thus largely able to maintain the identical optimal speed.

4.3.2 | Results comparison with other similar research

A comparative study is also conducted to show the performance of different ideas on regulating vehicles upstream of the work zone. The EM, LM, and New England Merge (NEM) strategies as mentioned in Ren et al. (2020) are considered under different density, which varies from 1200 to 2000 vph with an increment of 400 vph.

Similar to the present paper, NEM also investigates the problem of setting some areas upstream of the work zone with different objectives. However, the fundamental ideas of the two studies are different. In their study, before entering the merging area, vehicles in both lanes are projected onto a single virtual lane, and all the distance headways are expected to be close to but greater than the safe distance. On the contrary, in our research, vehicles adjusted their positions according to the optimal solution with the purpose of making full use of spatial gaps. Here, we use the same setups as those in Ren et al. (2020), where a work zone on a two-lane highway is considered with the right lane blocked; 70% cars and 30% trucks are considered in the platoon. The speed limit is set as 70 km/h. Notably, in their research, the mean travel time (MTT) is selected as the measurement of effectiveness measured from 1720 m upstream of the work zone. The results are presented in

Table 7. The proposed platoon regulation algorithm shows the minimum MTT in all considered scenarios.

Compared with the NEM strategy, in the low or medium traffic volume environment (e.g., 1200 and 1600 vph), though the platoon regulation performs the best, the performance of the two strategies is quite similar. In the high traffic volume environment (e.g., 2000 vph), the proposed method in this paper outperforms other groups. As aforementioned, in the low or medium traffic volume environments, vehicles have more opportunities to naturally complete lane changing, while in the high traffic volume traffic environments, it may cause congestion spread upstream of the work zone without a proper control method, leading to decreased speed.

5 | CONCLUSION AND DISCUSSION

In this paper, we propose a cooperative control strategy to facilitate merging control when vehicles are approaching the blocked lane. The basic idea is to exploit the benefits of CV technology in regulating vehicle trajectories at a regulation area, which is set upstream of the work zone. The proposed strategy consists of two stages, which are the regulation and the merging stages. In the regulation stage, we develop a nonlinear model called the RLP mainly to increase the capacity of the normal lanes as well as minimizing the influence on normal vehicles. The nonlinear model is further refined to a linear model by the designed two-step algorithm. The output of the RLP is used as the input of the merging control model in the merging stage. The sorting algorithm is applied to find the final optimal merging trajectories. Numerical experiments are conducted to demonstrate the effectiveness of the proposed control model. The result of the case study indicates that the proposed method could significantly improve the capacity of work zones. The present study also shows the possibility of combining the proposed method with existing ramp metering methods. Clearly, different initial setups will lead to different results. Even though we endeavor to provide sensitive analysis for crucial variables, it is intractable to examine all parameters in a paper of reasonable length. In practice, engineers and traffic management departments can adjust those initial setups according to real data to better formulate treatments against emergency events.

We summarize the contributions of this research as follows:

(1) We divide the area upstream of the work zone into the regulation and the merging areas, and a proactive approach to regulate the cooperative vehicles upstream of the work zone is proposed.

(2) Both efficiency and safety issues are considered in the RLP model when vehicles travel across the regulation area.

(3) Different from the previous trajectory optimization studies, this study is carried out at nonrecurrent bottlenecks such as work zones or crash sites.

Several limitations of this study are notable. First, the proposed method relies on a 100% penetration rate of cooperative vehicles. Future studies are desired to address the problem of mixed platoons with noncooperative vehicles in which the present study can serve as a building block. Second, how to control the capacity upstream of the regulation area combined with the proposed model needs future investigations. Third, some safety issues such as the safety of the workforce in a work zone are ignored. Future studies are desired to consider more factors in the control framework. In addition, the proposed method cannot address fully congested scenarios that entail traffic management on a larger scale.

REFERENCES
Adeli, H., & Ghosh-Dastidar, S. (2004). Mesoscopic-wavelet freeway work zone flow and congestion feature extraction model. *Journal of Transportation Engineering*, *130*(1), 94–103.

Ali, Y., Zheng, Z., Haque, M. M., & Wang, M. (2019). A game theory-based approach for modelling mandatory lane-changing behaviour in a connected environment. *Transportation Research Part C: Emerging Technologies*, *106*, 220–242.

Beacher A. G., Fontaine M. D., Garber N. J. (2005). Field Evaluation of Late Merge Traffic Control in Work Zones. *Transportation Research Record: Journal of the Transportation Research Board*, *1911*, (1), 33–41. http://doi.org/10.1177/0361198105191100104.

Brockfeld, E., Centre, G. A., Skabardonis, A., & Wagner, P. (2003). Towards a benchmarking of microscopic. *Transportation Research Record: Journal of the Transportation Research Board*, *1852*(1), 124–129.

Castillo-Manzano J. I., Castro-Nuño M., López-Valpuesta L., & Vassallo F. V. (2019). The complex relationship between increases to speed limits and traffic fatalities: Evidence from a meta-analysis. *Safety Science*, *111*, 287–297. http://doi.org/10.1016/j.ssci.2018.08.030.

Chen, N., van Arem, B., Alkim, T., & Wang, M. (2020). A hierarchical model-based optimization control approach for cooperative merging by connected automated vehicles. *IEEE Transactions on Intelligent Transportation Systems*, 1–14. https://doi.org/10.1109/TITS.2020.3007647

Chien, C. C., Zhang, Y., & Lai, M. (1995). Regulation layer controller design for automated highway systems. *Mathematical and Computer Modelling*, *22*(4–7), 305–327.

Chin, E., Franzese, O., Greene, D., Hwang, H., & Gibson, R. (2002). Temporary losses of highway capacity and impacts on performance. *Applications of advanced technologies in transportation*. American Society of Civil Engineers.

Choudhary, P., Imprialou, M., Velaga, N. R., & Choudhary, A. (2018). Impacts of speed variations on freeway crashes by severity and vehicle type. *Accident Analysis and Prevention*, *121*, 213–222.

Chung, Y., & Recker, W. W. (2012). A methodological approach for estimating temporal and spatial extent of delays caused by freeway accidents. *IEEE Transactions on Intelligent Transportation Systems*, *13*(3), 1454–1461.

Du, B., Chien, S., Lee, J., & Spasovic, L. (2017). Predicting freeway work zone delays and costs with a hybrid machine-learning model. *Journal of Advanced Transportation*, *2017*, 1–8.

Duret, A., Wang, M., & Ladino, A. (2020). A hierarchical approach for splitting truck platoons near network discontinuities. *Transportation Research Part B: Methodological*, *132*, 285–302.

Fritzsche, H. T. (1994). A model for traffic simulation. *Traffic Engineering and Control*, *35*(5), 317–321.

Gartner, N., Messer, C., & Rathi, A. K. (2001). *Traffic flow theory: A state-of-the-art report*. Transportation Research Board.

Ghiasi, A., Hussain, O., Qian, Z. S., & Li, X. (2017). A mixed traffic capacity analysis and lane management model for connected automated vehicles: A Markov chain method. *Transportation Research Part B: Methodological*, *106*, 266–292.

Godbole, D. N., & Lygeros, J. (1994). Longitudinal control of the lead car of a platoon. *Proceedings of the American Control Conference*, *1*(4), 398–402.

Gurobi Optimization, Inc. (2014). *Gurobi optimizer reference manual*. http://www.gurobi.com

Hall, R. W. (1995). Longitudinal and lateral throughput on an idealized highway. *Transportation Science*, *29*(2), 118–127.

Hall, R. W., & Lotspeich, D. (1996). Optimized lane assignment on an automated highway. *Transportation Research Part C: Emerging Technologies*, *4*, 211–229.

Han, Y., Hegyi, A., Yuan, Y., & Hoogendoorn, S. (2017). Validation of an extended discrete first-order model with variable speed limits. *Transportation Research Part C: Emerging Technologies*, *83*, 1–17.

Han, Y., Ramezani, M., Hegyi, A., Yuan, Y., & Hoogendoorn, S. (2020). Hierarchical ramp metering in freeways: An aggregated modeling and control approach. *Transportation Research Part C: Emerging Technologies*, *11*, 1–19.

Hooshdar, S., & Adeli, H. (2004). Toward intelligent variable message signs in freeway work zones: Neural network model. *Journal of Transportation Engineering*, *130*(1), 83–93.

Hou, Y., Edara, P., & Sun, C. (2015). Traffic flow forecasting for urban work zones. *IEEE Transactions on Intelligent Transportation Systems*, *16*(4), 1761–1770.

Hu, X., & Sun, J. (2019). Trajectory optimization of connected and autonomous vehicles at a multilane freeway merging area. *Transportation Research Part C: Emerging Technologies*, *101*, 111–125.

Jiang, X., & Adeli, H. (2003). Freeway work zone traffic delay and cost optimization model. *Journal of Transportation Engineering*, *129*(3), 230–241.

Jiang, X., & Adeli, H. (2004a). Clustering-neural network models for freeway work zone capacity estimation. *International Journal of Neural Systems*, *14*(3), 147–163.

Jiang, X., & Adeli, H. (2004b). Object-oriented model for freeway work zone capacity and queue delay estimation. *Computer-Aided Civil and Infrastructure Engineering*, *19*(2), 144–156.

Jing, S., Hui, F., Zhao, X., Rios-Torres, J., & Khattak, A. J. (2019). Cooperative game approach to optimal merging sequence and on-ramp merging control of connected and automated vehicles. *IEEE Transactions on Intelligent Transportation Systems*, *20*(11), 4234–4244.

Kang, K. P., & Chang, G. L. (2009). Dynamic late merge control at highway work zones: Evaluation, observations, and suggestions. *Intelligent Transportation Society of America: 12th World Congress on Intelligent Transport Systems*, *9*, 5693–5704.

Karim, A., & Adeli, H. (2003). CBR model for freeway work zone traffic management. *Journal of Transportation Engineering*, *129*(2), 134–145.

Letter, C., & Elefteriadou, L. (2017). Efficient control of fully automated connected vehicles at freeway merge segments. *Transportation Research Part C: Emerging Technologies*, *80*, 190–205.

Liu, H., Kan, X. D., Shladover, S. E., Lu, X. Y., & Ferlis, R. E. (2018). Modeling impacts of cooperative adaptive cruise control on mixed traffic flow in multi-lane freeway facilities. *Transportation Research Part C: Emerging Technologies*, *95*, 261–279.

Matírnez A., Mántaras D. A., & Luque P. (2013). Reducing posted speed and perceptual countermeasures to improve safety in road stretches with a high concentration of accidents. *Safety Science*, *60*, 160–168. http://doi.org/10.1016/j.ssci.2013.07.003

McCoy, P. T., & Pesti, G. (2001). Dynamic late merge-control concept for work zones on rural interstate highways. *Transportation Research Record*, *1745*(1), 20–26.

Memarian, A., Rosenberger, J. M., Mattingly, S. P., Williams, J. C., & Hashemi, H. (2019). An optimization-based traffic diversion model during construction closures. *Computer-Aided Civil and Infrastructure Engineering*, *34*(12), 1087–1099.

Ntousakis, I. A., Nikolos, I. K., & Papageorgiou, M. (2016). Optimal vehicle trajectory planning in the context of cooperative merging on highways. *Transportation Research Part C: Emerging Technologies*, *71*, 464–488.

Panwai, S., & Dia, H. (2005). Comparative evaluation of microscopic car-following behavior. *IEEE Transactions on Intelligent Transportation Systems*, *6*(3), 314–325.

Papageorgiou, M., Hadj-Salem, H., & Jean-Marc, B. (1990). Alinea. A local feedback control law for on-ramp metering. *Transportation Research Record*, *1320*, 194–198.

Papageorgiou, M., Papamichail, I., Spiliopoulou, A. D., & Lentzakis, A. F. (2008). Real-time merging traffic control with applications to toll plaza and work zone management. *Transportation Research Part C: Emerging Technologies*, *16*(5), 535–553.

Ren, T., Xie, Y., & Jiang, L. (2020). New England merge: A novel cooperative merge control method for improving highway work zone mobility and safety. *Journal of Intelligent Transportation Systems: Technology, Planning, and Operations*, *0*(0), 1–15.

Scarinci, R., Hegyi, A., & Heydecker, B. (2017). Definition of a merging assistant strategy using intelligent vehicles. *Transportation Research Part C: Emerging Technologies*, *82*, 161–179.

Sun, C., Pei, X., Hao, J., Wang, Y., Zhang, Z., & Wong, S. C. (2018). Role of road network features in the evaluation of incident impacts on urban traffic mobility. *Transportation Research Part B: Methodological*, *117*, 101–116.

Tarko, A. P., Kanipakapatnam, S. R., & Wasson, J. S. (1998). Modeling and optimization of the Indiana lane merge control system on approaches to freeway work zones. *Joint Transportation Research Program*, 345. https://doi.org/10.5703/1288284313469

Tsao, H. S. J., Hall, R. W., & Chatterjee, I. (1997). Analytical models for vehicle/gap distribution on automated highway systems. *Transportation Science*, *31*(1), 18–33.

Wang, X., Fan, T., Li, W., Yu, R., Bullock, D., Wu, B., & Tremont, P. (2016). Speed variation during peak and off-peak hours on urban arterials in Shanghai. *Transportation Research Part C: Emerging Technologies*, *67*, 84–94.

Wang, X., Zhou, Q., Quddus, M., Fan, T., & Fang, S. (2018). Speed, speed variation and crash relationships for urban arterials. *Accident Analysis and Prevention*, *113*, 236–243.

Wang, Z., Zhao, X., Xu, Z., Li, X., & Qu, X. (2020). Modeling and field experiments on autonomous vehicle lane changing with surrounding human-driven vehicles. *Computer-Aided Civil and Infrastructure Engineering*, 1–13. https://doi.org/10.1111/mice.12540

Wu, J., Ahn, S., Zhou, Y., Liu, P., & Qu, X. (2021). The cooperative sorting strategy for connected and automated vehicle platoons. *Transportation Research Part C: Emerging Technologies*, *123*, 102986.

Wu, J., Kulcsár, B., Ahn, S., & Qu, X. (2020). Emergency vehicle lane pre-clearing: From microscopic cooperation to routing decision making. *Transportation Research Part B: Methodological*, *141*, 223–239.

Xu, Z., Wang, Y., Wang, G., Li, X., Bertini, R. L., Qu, X., & Zhao, X. (2020). Trajectory optimization for a connected automated traffic stream: Comparison between an exact model and fast heuristics. *IEEE Transactions on Intelligent Transportation Systems*, *99*, 1–10.

Yang, N., Chang, G. L., & Kang, K. P. (2009). Simulation-based study on a lane-based signal system for merge control at freeway work zones. *Journal of Transportation Engineering*, *135*(1), 9–17.

Zheng, H., Nava, E., & Chiu, Y. C. (2014). Measuring networkwide traffic delay in schedule optimization for work-zone planning in urban networks. *IEEE Transactions on Intelligent Transportation Systems*, *15*(6), 2595–2604.

Zheng, Z. (2014). Recent developments and research needs in modeling lane changing. *Transportation Research Part B: Methodological*, *60*, 16–32.

Zheng, Z., Ahn, S., & Monsere, C. M. (2010). Impact of traffic oscillations on freeway crash occurrences. *Accident Analysis and Prevention*, *42*(2), 626–636.

Zheng, Z., & Sarvi, M. (2016). Modeling, calibrating, and validating car following and lane changing behavior. *Transportation Research Part C: Emerging Technologies*, *71*, 182–183.

Zhong, Z., & Lee, J. (2019). The effectiveness of managed lane strategies for the near-term deployment of cooperative adaptive cruise control. *Transportation Research Part A: Policy and Practice*, *129*, 257–270.

Zhou, Y., & Ahn, S. (2019). Robust local and string stability for a decentralized car following control strategy for connected automated vehicles. *Transportation Research Part B: Methodological*, *125*, 175–196.

Zhou, Y., Chung, E., Bhaskar, A., & Cholette, M. E. (2019). A state-constrained optimal control based trajectory planning strategy for cooperative freeway mainline facilitating and on-ramp merging maneuvers under congested traffic. *Transportation Research Part C: Emerging Technologies*, *109*, 321–342.